LA-UR-19-29255
Approved for public release; distribution is unlimited.

Title: FY19 Summary Report: Thermal and Mechanical Characterization of DAAF and LAX-133

Author(s): Thompson, Darla Graff
DeLuca, Racci
Woznick, Caitlin Savanna

Intended for: Report

Issued: 2019-09-16

FY19 Summary Report: Thermal and Mechanical Characterization of DAAF and LAX-133

Darla Graff Thompson, Caitlin Woznick, Racci DeLuca
High Explosives Thermal and Mechanical Characterization Team, M-7, Los Alamos National Laboratory
09 September 2019

We have performed a series of thermal and mechanical tests to characterize the high explosive 3,3'-diamino-4,4'-azofurazan (DAAF), as well as the formulated version LAX-133 (97 wt% DAAF and 3 wt% FK-800 binder, now also referred to as PBX 9701; for clarity in this report, we will use the name LAX-133 which is what the formulated material was called at the time this work was performed.) Specifically, we have used axially die-pressed cylinders (with no further machining) of neat DAAF and of LAX-133 to make measurements of compressive strength, Brazil disk, coefficient of thermal expansion (CTE), as well as irreversible volume expansion with thermal cycling (ratchet growth).

In this study, the LAX-133 used was lot LAX-133-37-2-24-15 (Material Safety Release WX-7-AC-15-023 from March 2015), and the DAAF used was lot 500-45-36. Figure 1 shows the hand-measured specimen densities vs. arbitrary specimen number. The target density was 1.690 g/cm3.

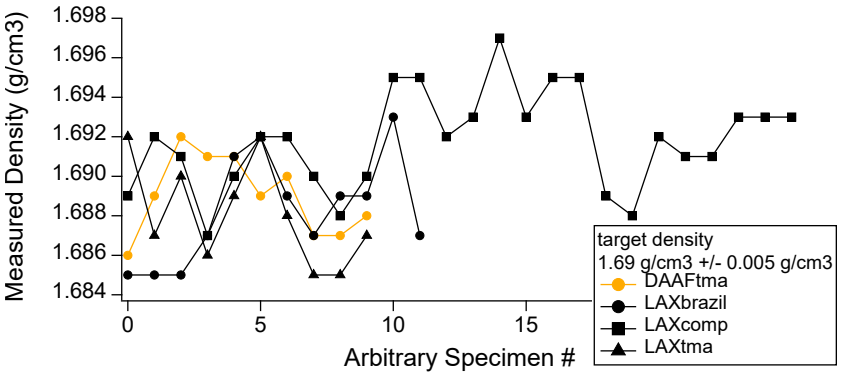

Figure 1: Hand-measured specimen densities, see legend for specimen identification.

Compression specimens were tested to failure on an Instron 5567 with a Bemco environmental chamber (TA-9, Bldg 33) to control the temperature. The specimens are 0.75 inches long and 0.5 inches in diameter. Oppositely-mounted knife-edge extensometers were used to measure strain. The raw stress-strain curves for compression are plotted in Figure 2. Colors in this figure indicate test temperature (50, 20, -15°C) while line types indicate crosshead speed (strain rate). The general trends are consistent with PBX formulations, namely that lower temperatures and faster strain rates give rise to higher failure stress.

In order to compare the mechanical response of two materials, we reduce the raw stress-strain curves in Figure 2 to three compression parameters, plotted versus log(strain rate) on the left-hand-side of Figure 3. Symbol colors still indicate temperature. The compression parameters are Stress Maximum at failure (top graph), Strain at Stress Maximum (center graph), and the Modulus at 25% of Stress Maximum (bottom graph). Following a Time-Temperature Superposition protocol [1] that we have successfully applied to many other PBXs, we determined a by-eye best-fit shift factor of A = 7.5°C/(decade strain rate). This shift factor effectively says that a 7.5°C reduction in temperature is

equivalent to a decade increase in strain rate. On the right-hand-side of Figure 3 are shown the Master Curves at 20°C Equivalence, following the Time-Temperature shift.

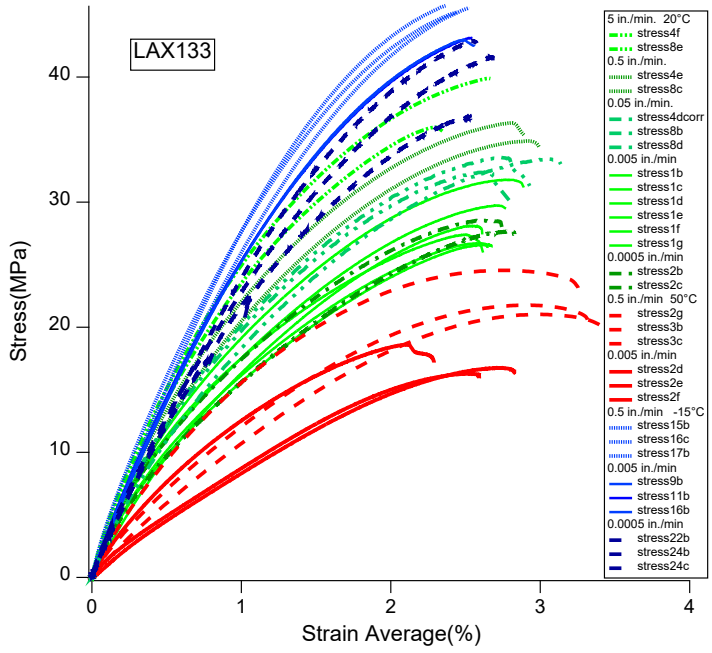

Figure 2: Raw stress-strain compression curves for LAX-133, see legend for test condition.

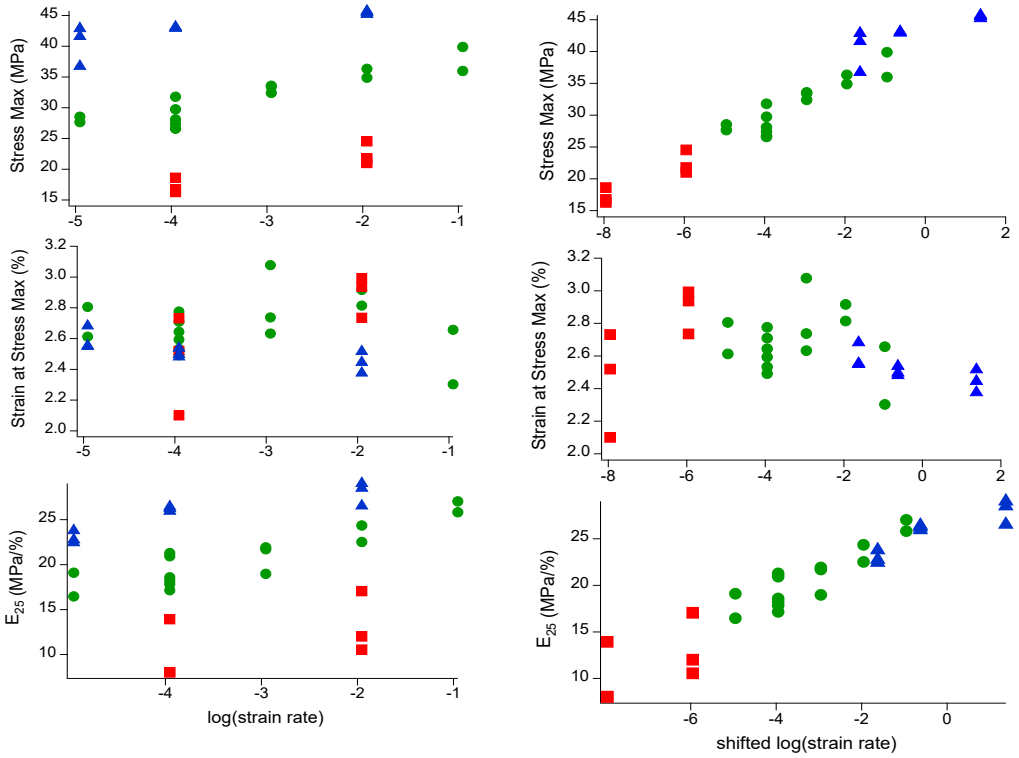

Figure 3: (Left) Compression parameters plotted versus strain rate for the raw data in Figure 2 (same color coding for temperature). (Right) Compression parameters as 20°C Equivalence Master Curves after a Time-Temperature superposition using 7.5°C/(decade strain rate).

In Figure 4, we plot the LAX-133 compression Master Curves from Figure 3 with the equivalent Master Curves of LX-07, an HMX-based booster material with Viton-A as binder. At low strain rates (<100 s-1), the modulus (stiffness) of the two materials is very similar; at faster rates, the glass transition of Viton causes the modulus to increase greatly. At the lower strain rates, the failure strength of LAX-133 exceeds that of LX-07, as does the strain at failure. More testing of both materials over a broader set of conditions would fill in the ill-determined regions of the Master Curves.

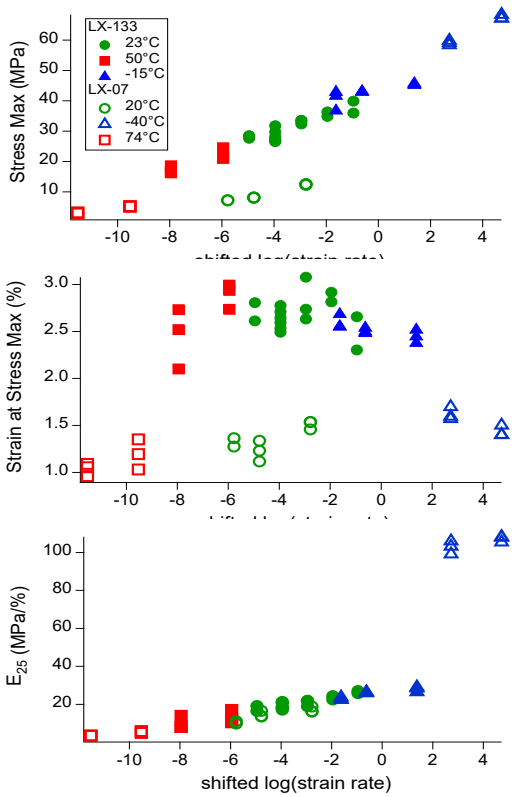

Figure 4: Compression Master Curves (after Time-Temperature shifiting) of LAX-133 and LX-07, both at 20°C equivalence.

In Figure 5 are shown photos of two different post-compression LAX-133 specimens. In the left image, we see that a fragment of the cylinder popped off during testing, and occurred at an internal defect of the cylinder. The fragment indicates a very brittle failure. Likewise, the image on the right shows a post-test specimen still mounted inside the extensometers, and shows significant fragmentation associated with brittle failure.

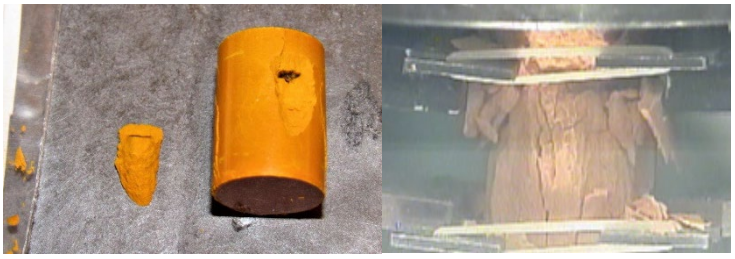

Figure 5: Two post-test photographs of LAX-133 compression specimens showing brittle failure.

Brazil disk tests were also performed on LAX-133 specimens using the Instron and Bemco environmental chamber. The specimens are 4 mm thick and 19.05 mm in diameter. In these tests, LAX-133 disks are compressed vertically across the diameter, (see the pre-test photo, Figure 6, left). In this configuration, the vertical compressive stress results in a horizontal tensile stress, and the

specimen should fail in tension with a crack opening at the center of the disk. However, due to the extremely brittle nature of LAX-133 (and consistent with other brittle formulations tested by us such as Comp B and Cyclotol), multiple vertical cracks open across the disk during failure, and the test is no longer considered valid.

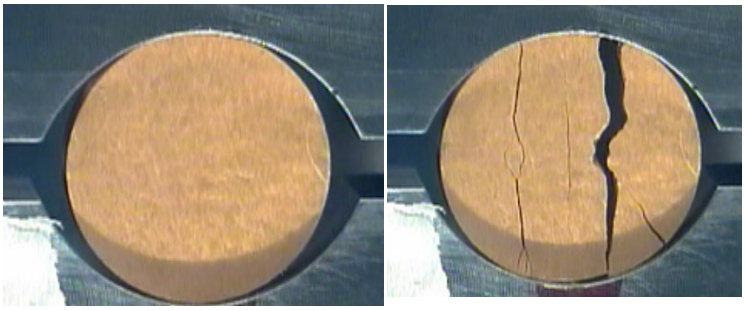

Figure 6: (left) Pre-test and (right) post-test images of a Brazil disk test showing multiple tensile cracks across the disk face.

The raw Brazil disk data are plotted as load versus extension in Figure 7. Note that a decreasing temperature results in increased stiffness with higher failure strength and strain, similar to compression discussed above.

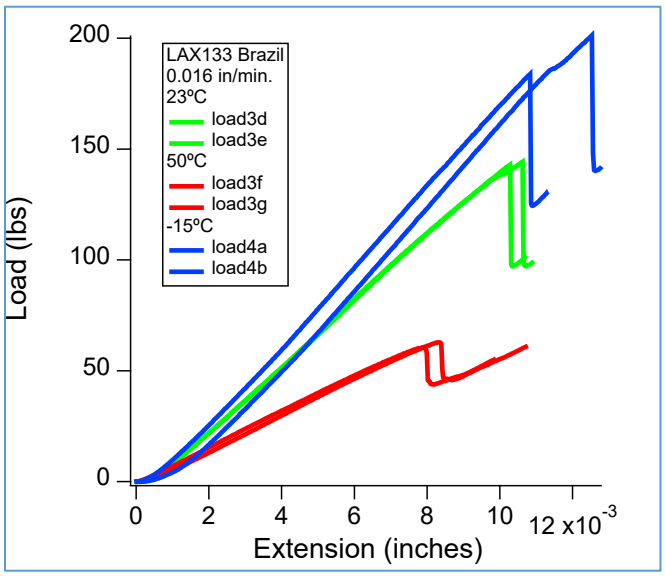

Figure 7: Raw Load-Extension data for LAX-133 Brazil Disk Tests. See legend for test conditions.

The coefficient of thermal expansion (CTE) of DAAF and LAX-133 was measured using a TA Instruments Q400 Thermal-Mechanical Analyzer (TMA). The specimens are 5 mm diameter by 5 mm long with thermal ramp rates of 1°C/min to ensure thermal equilibrium. These CTE data are plotted in Figure 8 as strain (%) versus temperature, along with TATB that is also as-pressed and PBX 9502 that has been machined out of an isostatically-pressed charge. LAX-133 and PBX 9502 both have FK-800 as the binder whose glass transition is at 28°C. There may be a slight upturn of the CTE near this point for these binder-containing materials, but the effect is slight.

To further the comparison with TATB and PBX 9502 [2], we performed DAAF and LAX-133 thermal cycling experiments using the TMA to look for evidence of irreversible volume expansion (ratchet growth). Ratchet growth is an undesirable characteristic of TATB believed to arise from a

strongly anisotropic thermal expansion in its single crystals. We had heard rumor that DAAF may also have this characteristic. In Figure 9, thermal expansion data are plotted similar to that shown in Figure 8, however, now for many repeated thermal cycles over the given range (-53 to 153C). A linear material, such as aluminum or copper, would simply show a single line in Figure 9, as the response simply moved up and down on it. Ratchet growth is observed as the CTE "ratchets up" with each new cycle, its strain increasing irreversibly. The data in Figure 9 show us that the ratchet growth of TATB over this range is the most significant, however, PBX 9502, DAAF and LAX-133 also show some ratchet growth.

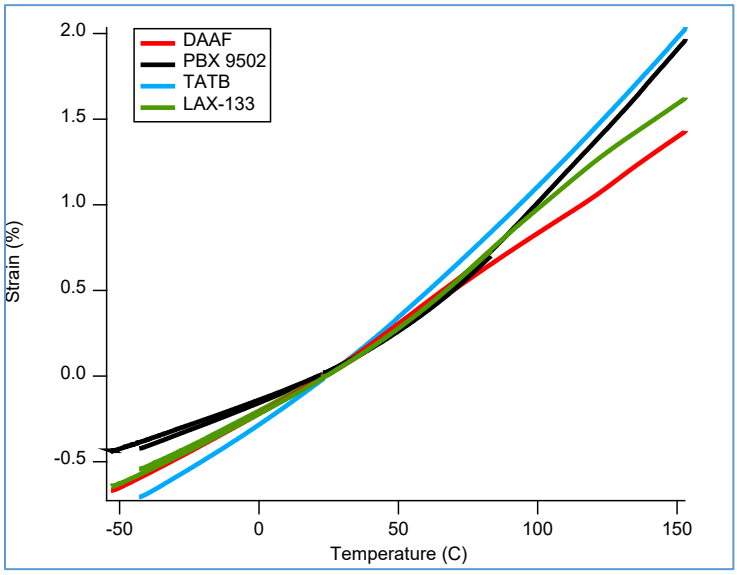

Figure 8: Thermal expansion plots from the TMA.

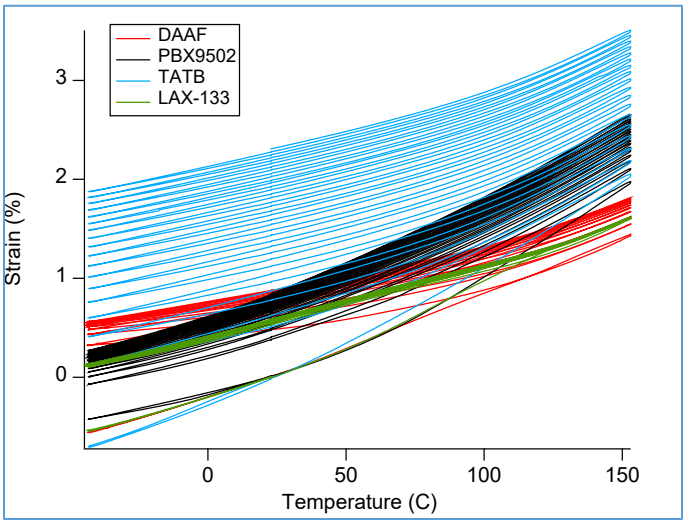

Figure 9: Thermal expansion plots from the TMA for many hot-cold thermal cycles. Irreversible volume expansion is observed.

In Figure 10 we show the analysis of ratchet growth data for DAAF, LAX-133, TATB and PBX 9502. Data are plotted as the irreversible strain per hot-cold cycle ($\Delta\varepsilon$) versus the accumulated strain per hot-cold cycle ($\Sigma\Delta\varepsilon$). In these graphs, each data point corresponds to the irreversible growth measured at 23°C following one complete cycle that goes cold then hot. Note the different axis scales for the different temperature ranges. Based on the data as presented in Figure 10, we would conclude that indeed DAAF and a DAAF-FK800 formulation do demonstrate ratchet growth behavior somewhat

similar to TATB and a TATB-FK800 formulation, however, the same data are analyzed further in Figure 11 where interesting differences are observe.

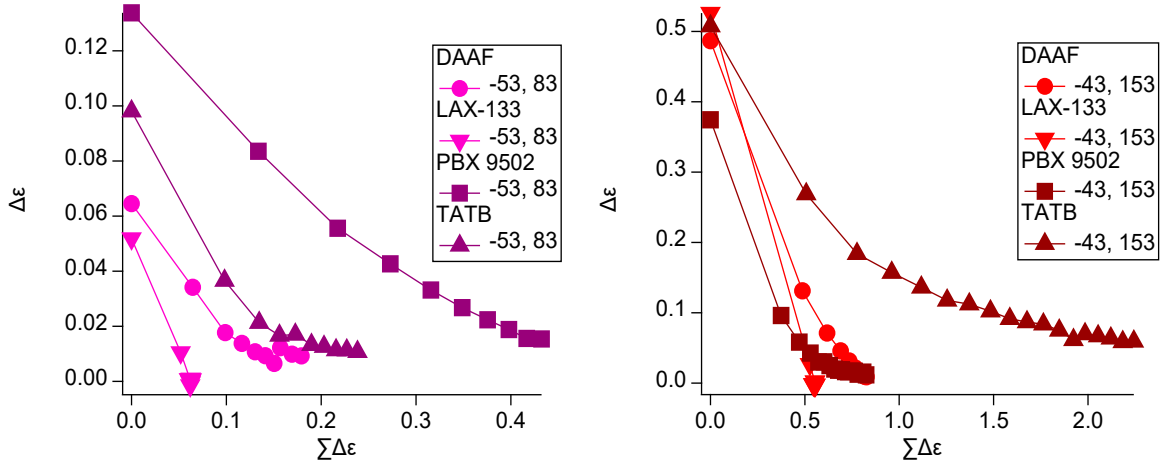

Figure 10: Ratchet growth analysis of TMA data, the irreversible strain per hot-cold cycle ($\Delta\varepsilon$) versus the accumulated strain per hot-cold cycle ($\Sigma\Delta\varepsilon$). See legend for specimen identification. (Left) Data for thermal cycles between -53 and 83°C and (right) for thermal cycles between -43 and 153°C.

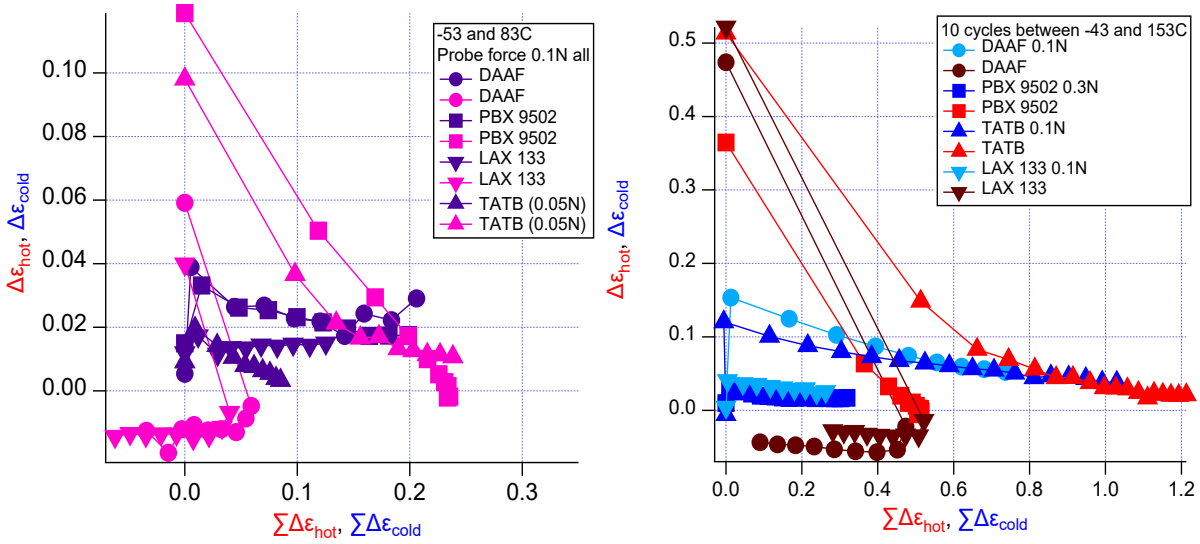

Figure 11: Similar to the data in Figure 10 except that now the strain contributions of the cold cycles are separated from those of the hot cycles. The irreversible strain of each hot cycle ($\Delta\varepsilon_{hot}$) is plotted versus the accumulated strain per hot-cold cycle ($\Sigma\Delta\varepsilon_{hot}$). The same is done for strain of the cold cycles. See legend for specimen identification. (Left) Data for thermal cycles between -53 and 83°C and (right) for thermal cycles between -43 and 153°C.

In Figure 11, the combined cold-hot strains plotted in Figure 10 are now separated into their hot cycle and cold cycle contributions. We have found this to be a useful analysis in the characterization of TATB and PBX 9502. In Figure 11, the left plot contains data for the -53 to 83°C cycles, and the right contains data for the -43 to 153°C cycles. The observations are similar for each, but we will discuss the data over the larger temperature range where the effect is greater and clearer. The behavior of the cold

cycles (blue-colored symbols) is very similar (and even nearly identical) for TATB and DAAF, and also for LAX-133 and PBX 9502. Specifically the growth of subsequent cycles continues but is slowly tapering off (what is also interesting, and not shown here, is that if cold cycles are run alone--- without the intervening hot cycles--- their growth contributions are exceedingly small and taper to nothing after only a couple of cycles). It is the behavior of the hot cycles (red-colored symbols) where we see very different behavior in DAAF and LAX-133 when compared with TATB and PBX 9502. The DAAF-containing specimens start out the first hot cycle with large irreversible strain, comparable to that observed for TATB, however, by the second hot cycle, the strain contributions begin to go negative. The specimen is no longer expanding but now contracting (or creeping, recall that there is a very slight load of 0.1N applied by the TMA probe). We have previously seen behavior somewhat similar when we performed thermal cycling experiments on pressed pellets of dry PETN, and these results are included in Figure 12, along with the results from this study. Here we plot the accumulating strain per cold-hot cycle (back to Figure 10), and we see the clear difference of materials that ratchet grow (TATB-based) versus materials that shrink or creep (PETN). From the insight of Figure 11, we understand that the DAAF and LAX-133 behavior is complex and kind of "in the middle." Figure 12 shows that for DAAF, the cold-hot cycles result in overall growth with repeated cycles. For LAX-133, there is initial growth but then the warm response dominates and subsequent cycles result in shrinking or creep of the material.

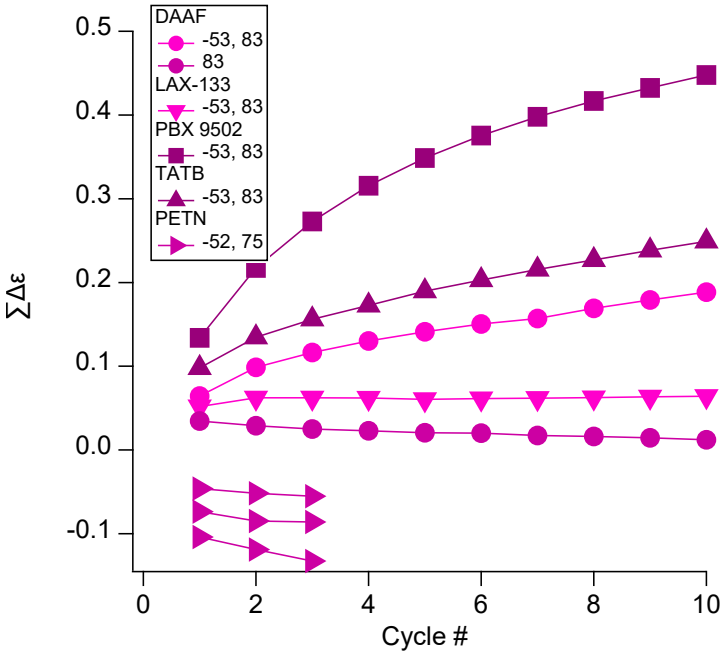

Figure 12: Accumulated strain is plotted versus combined cold-hot cycle number. See legend for specimen identification.

For a final bit of insight, we performed a series of TMA tests where the specimens were taken to high temperatures and held for 20 hours while the strain was monitored. The data are shown in Figure 13. Note that the TATB and PBX 9502 specimens were held at 113°C with a probe force of 0.3N for 20 hours. The DAAF and LAX-133 were held at 83°C with a probe force of 0.1N for 20 hours. Even with a lower probe force and lower temperature, the DAAF and LAX-133 creeped or shrank during the test compared with PBX 9502, and especially with TATB, which showed the well-characterized effect of isothermal ratchet growth [3].

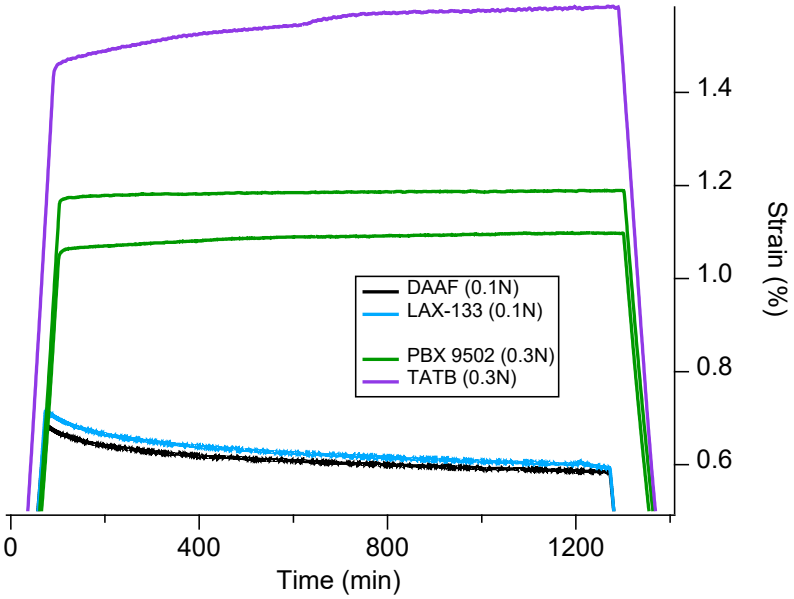

Figure 13: Isothermal tests on the TMA, specimens were taken to temperature and held for 20 hours. DAAF and LAX-133 were taken to 83°C, while the TATB and PBX 9502 were taken to 113°C.

We conclude by saying that DAAF- and DAAF-containing PBXs do show signs of ratchet growth, but also demonstrate other complex behavior upon thermal cycling that is not well-understood by us and is likely not entirely desirable. Further characterization should be performed to have a better idea of what is unique about this material with respect to thermal cycling and to high-temperature soaks.

References

[1] "Time-temperature analysis of plastic-bonded explosives PBX 9501 and PBX 9502 in tension and compression," Darla Graff Thompson, Racci DeLuca, Geoff W, Brown, Journal of Energetic Materials, 30(4), 2012, 299-323. LA-UR 11-07068.

[2] "Thermal Cycling and Ratchet Growth of TATB and PBX 9502," Darla Graff Thompson, Caitlin Woznick, Racci DeLuca, Propellants, Explosives and Pyrotechnics, 2019, 44(7), 850-857, LA-UR 18-30374.

[3] "Time-Evolution of TATB-Based Irreversible Thermal Expansion (Ratchet Growth)," Darla Graff Thompson, Ricardo B. Schwarz, Geoff W. Brown, Racci DeLuca, Propellants Explos. Pyrotech., 40, 558 - 565, 2015 (LA-UR-14-26994).